Unprecedented High Probe-Reported Polarity of Deep Eutectic Solvents Composed of Lanthanide Salts and Urea

Anushis Patra , Vaishali Khokhar , Siddharth Pandey *

Posted Date: 6 May 2024

doi: 10.20944/preprints202405.0237.v1

Keywords: deep eutectic solvent; hydrated lanthanide salts; Urea; dipolarity/polarizability (π*); pyrene-1-carboxaldehyde; Nile red; aggregates; pyranine

 doi:10.20944/preprints202405.0237.v1

Article

Unprecedented High Probe-Reported Polarity of Deep Eutectic Solvents Composed of Lanthanide Salts and Urea

Anushis Patra, Vaishali Khokhar and Siddharth Pandey *

Department of Chemistry, Indian Institute of Technology Delhi, Hauz Khas, New Delhi – 110016, India; anuchemistry2019@gmail.com (A.P.); vaishalikhokhar57@gmail.com (V.K.)
* Correspondence: sipandey@chemistry.iitd.ac.in; Phone: +91-11-26596503, Fax: +91-11-26581102

Abstract: Deep eutectic solvents (DESs) have emerged as viable alternatives to the toxic organic solvents. The most intriguing aspect of these solvents is perhaps the widely varying physicochemical properties emerging from the changes in the constituents that form DESs along with their composition. Based on the constituents, a DES can be hydrophilic/polar or hydrophobic/non-polar rendering vastly varying spectrum of polarity a possibility. DESs formed by mixing urea (U) with hydrated lanthanide salts, lanthanum nitrate hexahydrate (La : U), cerium nitrate hexahydrate (Ce : U), and gadolinium nitrate hexahydrate (Gd : U), respectively, exhibit very high polarity as manifested via probe-reported empirical parameters dipolarity/polarizability (π^*). The highest π^* of 1.70 exhibited by the DES (Gd : U) in 1 : 2 molar ratio is unprecedented. The π^* ranges from 1.50 to 1.70 for these DESs, which is almost the highest reported for any solvent system. The π^* decreases with increasing urea in the DES, however, the anomalous trends in H-bond donating acidity (α) and H-bond accepting basicity (β) appear to be due to the hydrated water of the lanthanide salt. The emission band maxima of fluorescence probe of "effective" dielectric constant (ε_{eff}) of the solubilizing media, pyrene-1-carboxaldehyde (PyCHO), in salt-rich DESs reflect higher cybotactic region dipolarity than even that offered by water. Probe Nile red aggregates readily in these DESs to form non-fluorescent H-aggregates; a characteristic of highly polar solvents. Behavior of probe pyranine also corroborates these outcomes as the (lanthanide salt : urea) DES system supports the formation of deprotonated form of the probe in the excited-state. The (lanthanide salt : urea) DES system offers solubilizing media of exceptionally high polarity, which is bound to expand their application potential.

Keywords: deep eutectic solvent; hydrated lanthanide salts; urea; dipolarity/polarizability (π^*); pyrene-1-carboxaldehyde; Nile red; aggregates; pyranine

1. Introduction

Currently, the most emerged and prominent solvent class belonging to the area of green chemistry is arguably comprises of deep eutectic solvents (DESs). DESs are usually obtained by simply mixing two or more constituents in a particular molar ratio followed by gentle heating. In DESs, the thermodynamics of mixing ensures significant lowering of the normal freezing point as compared to those of the individual constituents [1–5]. While application potential of DESs lies in their environmentally-benign nature with negligible toxicity along with the low-cost of the constituents and preparation, the escalated interest in academia is due to the fact that a wide variety of physicochemical properties of these neoteric media are possible based on the identity of the constituents and their composition used to prepare these solvents [6–10]. Based on the chemical nature of the constituents, the DESs are divided into several classes. In the formation of DESs, usually one component behaves as an H-bond donor (HBD) and the other as an H-bond acceptor (HBA)

 doi:10.20944/preprints202405.0237.v1

leading to extensive H-bonding and other interactions (van der Waals, electrostatic, etc.) resulting in liquid state under wide range of temperature and pressure [1–5].

DESs have been investigated extensively not only for their applications but also for their physicochemical properties. Consequently, among other classifications, DESs may also be divided into 'hydrophilic' and 'hydrophobic' with 'hydrophilic' DESs offering complete water-miscibility and relatively high polarities [11,12]. DESs composed of mixing a quaternary ammonium salt as HBA with a suitable HBD have shown to possess relatively high polarity (as reported by several solvatochromic probes) in comparison to common solvents [13]. Extensive research has been carried out to characterize metal-based DESs by understanding their physicochemical properties with variation in the identity and composition of the constituents [14,15]. Kamlet-Taft parameters, in this context, have afforded understanding of the H-bonding interactions that occur inside the hydrated metal salt-based DESs [16–19]. Herein, we report our findings of exceptionally high probe-reported polarity exhibited by a set of type IV DESs constituted of hydrated lanthanide metal salts as HBA and urea as prototypical HBD [14]. These DESs have recently shown to support probe aggregation at unprecedented low concentrations [20]. Specifically, three (3) HBD urea-based DESs containing HBA metal salts lanthanum nitrate hexahydrate (La : U), cerium nitrate hexahydrate (Ce : U), and gadolinium nitrate hexahydrate (Gd : U), respectively, are found to exhibit some of the highest probe-reported polarities in terms of empirical Kamlet-Taft parameters of dipolarity/polarizability (π^*) [21] and HBD acidity (α) [22] along with E_T values [22]. The highly dipolar nature of the solubilization microenvironment offered by these DESs was further emphasized by the cybotactic region dipolarity of several fluorescence probes.

2. Materials and Methods

Hydrated metal salts [lanthanum nitrate hexahydrate (La), cerium nitrate hexahydrate (Ce), and gadolinium nitrate hexahydrate (Gd)] and urea were chosen as the DES constituents and were obtained with the highest purity ≥ 99 % from Sigma-Aldrich and SRL Enterprises respectively. *N*,*N*-Diethyl-4-nitroaniline (DENA), 4-nitroaniline (NA) (Figure 1) were used as absorbance probes in the work. DENA and NA were obtained from Frinton Laboratories and Spectrochem Co. Ltd., respectively, while Pyridin-*N*-oxide (PyO, 95%), Pyrene-1-carboxyldhyed (PyCHO, 99%), 9-diethylamino-5-benzo[a]phenoxazinone (Nile red, ≥98%, HPLC), and 8-hydroxypyrene-1,3,6-trisulfonic acid (pyranine, 99%) (Figure 1) were purchased from Sigma-Aldrich. These were used without any further purification.

DESs (La : U), (Ce : U), and (Gd : U) were prepared by simple mixing of the lanthanide salts (all ≥ 99+% purity) with urea (> 99.9% purity) at permissible (in the context of DES formation) molar composition ranges (1 : 3 to 1 : 7 for La : U, 1 : 3.5 to 1 : 7 for Ce : U, and 1 : 2 to 1 : 7 for Gd : U). At several compositions, simple mixing of the two solid constituents resulted in liquid state DESs under ambient conditions (no heating was required). All uv-vis molecular absorbance and fluorescence as well as NMR spectroscopic probes were dissolved in the DES and the probe responses were acquired using adequate sampling and data collection techniques using appropriate instrumentation.

Stock solutions of probes were prepared by dissolving precalculated amount of the respective probe in ethanol and stored at 4 ± 1°C in pre-clean brown amber glass vials. Mettler-Toledo AB104-S balance was used to weigh the proper amount of probe with an accuracy of ± 0.0001 g. A prerequisite amount of the prepared stock solution was taken in a 1 cm^2 quartz cuvette. Grade 1 nitrogen gas was used to evaporate the ethanol. The UV-visible absorbance spectra of all samples were collected by using Lambda 35 double beam spectrophotometer (purchased from PerkinElmer), containing with photomultiplier tube (PMT) detector and flexible with deuterium and a Xe lamp as a light source. The required amount of the DES under investigation was transferred to the cuvette. Dissolution of the probes in DESs were confirmed using the linearity of the absorbance versus the concentration plot. The ^{13}C of 250 mM PyO dissolved in La : U based DESs was obtained on Brucker 500 MHz (DPX-500) NMR Spectrometers. $CDCl_3$ was used as internal reference, sample was taken in the sealed capillary inside the same NMR tube (consists of $CDCl_3$). The steady-state fluorescence spectra were obtained using a FLS1000 spectrometer with emission monochromators (STGM325-M) and grating

 doi:10.20944/preprints202405.0237.v1

excitation (STGM325-X) containing a 450 W xenon arc lamp as the radiation source, a red PMT detector, and a temperature-controller (a Quantum Northwest Luma 40). The spectrometer was bought from Edinburgh Instruments, Ltd. Appropriate blank was subtracted from the emission and excitation spectra before analysis. Data analysis was accomplished using SigmaPlot v14.5. A Horiba-Jobin Yvon Fluorocube time-correlated single-photon counting (TCSPC) fluorimeter was used to measure the fluorescence lifetime of the selected probe. Samples were also characterized through Attenuated Total Reflectance-Fourier Transform infrared (ATR-FTIR) absorbance data which were acquired on a double-beam spectrophotometer (Agilent Technologies Cary 660 ATR) from 4000 to 400 cm^{-1}.

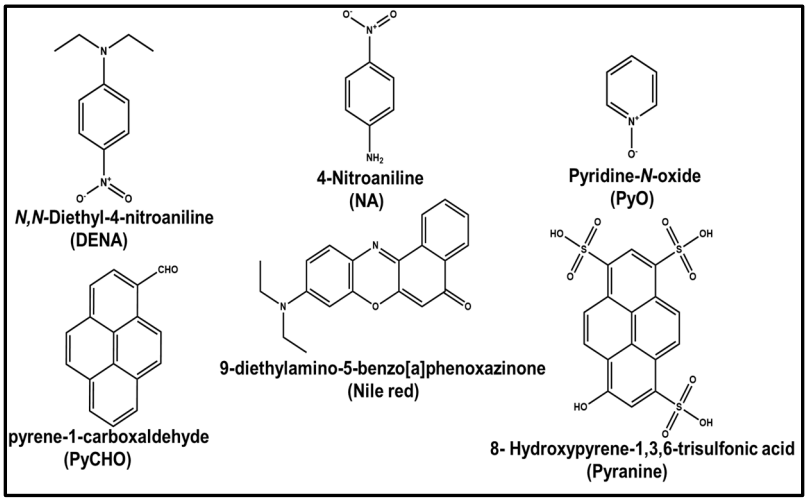

Figure 1. Molecular structures of the solvatochromic probes used in this work.

3. Results and Discussion

DESs (La : U), (Ce : U), and (Gd : U) were prepared by simple mixing of the lanthanide salts (all ≥ 99+% purity) with urea (> 99.9% purity) at permissible (in the context of DES formation) molar composition ranges (1 : 3 to 1 : 7 for La : U, 1 : 3.5 to 1 : 7 for Ce : U, and 1 : 2 to 1 : 7 for Gd : U). At several compositions, simple mixing of the two solid constituents resulted in liquid state DESs under ambient conditions (no heating was required). All uv-vis molecular absorbance and fluorescence as well as NMR spectroscopic probes were dissolved in the DES and the probe responses were acquired using adequate sampling and data collection techniques using appropriate instrumentation.

Well-established uv-vis molecular absorbance probes, *N*,*N*-diethyl-4-nitroaniline (DENA) [21] and 4-nitroaniline (NA) [23] (Figure 1), were employed to obtain dipolarity/polarizability (π^*) and H-bond accepting (HBA) basicity (β) of the three DESs at several different compositions using the following expressions:

$$\boldsymbol{\pi^* = 8.649 - 0.314\bar{\upsilon}_{DENA}} \quad (1)$$

$$\beta = \boldsymbol{-0.357\bar{\upsilon}_{NA} - 1.176\pi^* + 11.12} \quad (2)$$

where $\bar{\upsilon}_{DENA}$ and $\bar{\upsilon}_{NA}$ are the lowest energy absorbance band maxima of the probes DENA and NA, respectively, in kK units (1000 cm^{-1} = 1 kK). Our attempts to obtain E_T values [that subsequently afford HBD acidity (α)], using Reichardt's betaine dyes 30 and 33, the most-used probes for the purpose, were futile as either these dyes were insoluble in our DESs or due to the protonation of $–O^-$ these dyes did not exhibit lowest-energy intramolecular charge-transfer absorbance bands. Schneider et al. [24] used pyridine-*N*-oxide (PyO) (Figure 1) as a probe to characterize HBD acidity (α) of several solvents using ^{13}C NMR chemical shifts using the following equations:

$$\boldsymbol{\alpha_{24} = 2.32 - 0.15 \times d_{24}} \quad (3)$$

Preprints.org (www.preprints.org) | NOT PEER-REVIEWED | Posted: 6 May 2024 doi:10.20944/preprints202405.0237.v1

where d_{24} is the difference (in ppm) of the ^{13}C NMR chemical shifts ($\boldsymbol{\delta}$) of carbon 2 with respect to that of carbon 4 of PyO. The correlation between α thus estimated and the α from Reichardt's dye ($\boldsymbol{\alpha_{RD}}$) was established by Freire [22] group recently:

$$\boldsymbol{\alpha_{24} = 0.88 \times \alpha_{RD}} \quad (4)$$

supporting the suitability of PyO as an alternative probe to characterize HBD acidity of the solvents. It was further shown that $\boldsymbol{E_T(30)}$ [22] and $\boldsymbol{E_T^N}$ [22] single parameter polarity scales can be subsequently obtained using the following equations:

$$\boldsymbol{E_T(30) = (\alpha_{RD} + 2.03 + 0.72\,\pi^*)/\,0.0649} \quad (5)$$

and

$$\boldsymbol{E_T^N = (E_T(30) - 30.7)/\,32.4} \quad (6)$$

The absorbance spectra and the respective absorbance maxima of DENA and NA in all three DESs at all investigated compositions are presented in Figure S1 and Table S1, respectively (representative spectra within DESs (Gd : U) at 1 : 2 and 1 : 7 molar ratios are shown in Figure 2). With the increase in the amount of urea in all three DES systems, a significant hypsochromic shift in DENA wavelength maxima is clearly observed. While similar to DENA, the NA wavelength maxima does depend to some extent on the identity of the lanthanide metal, interestingly, contrary to DENA, the band maxima of NA are statistically the same irrespective of the amount of urea in the DES system. ^{13}C NMR scans of PyO within (La : U) at 1 : 3 and 1 : 7 molar ratios are presented in Figure 3 as representatives (others ratios are shown in Figure S2). It is to be noted that (Ce : U) based DESs appear to react with PyO, and due to high number of unpaired electrons in Gd, the ^{13}C NMR of PyO in (Ce : U) and (Gd : U) DESs could not be obtained. The values of empirical parameters π^*, β, α and $\boldsymbol{E_T^N}$, estimated from equations (1)-(6) for the applicable DES systems, are presented in Tables 1 and 2. A careful examination of the empirical parameters listed in Tables 1 and 2 reveals that π^*, $\boldsymbol{E_T^N}$, and α decrease while β increases monotonically as the relative amount of urea is increased within a DES system.

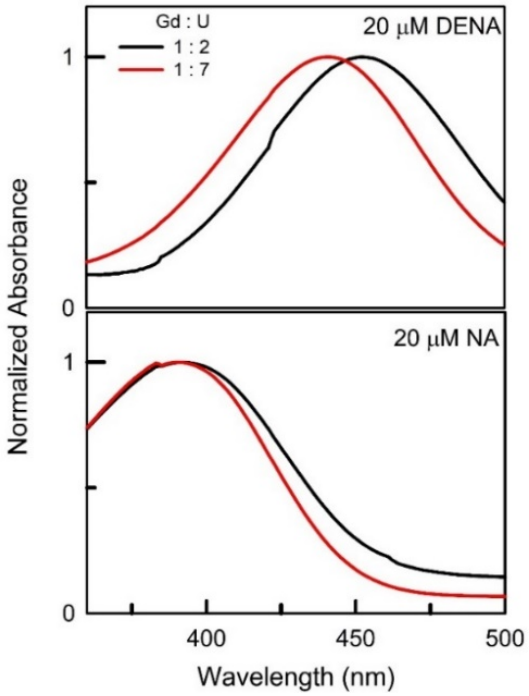

Figure 2. Representative absorbance spectra of 20 μM DENA and 20 μM NA within DESs (Gd : U) at 1 : 2 and 1 : 7 molar ratios.

Preprints.org (www.preprints.org) | NOT PEER-REVIEWED | Posted: 6 May 2024 doi:10.20944/preprints202405.0237.v1

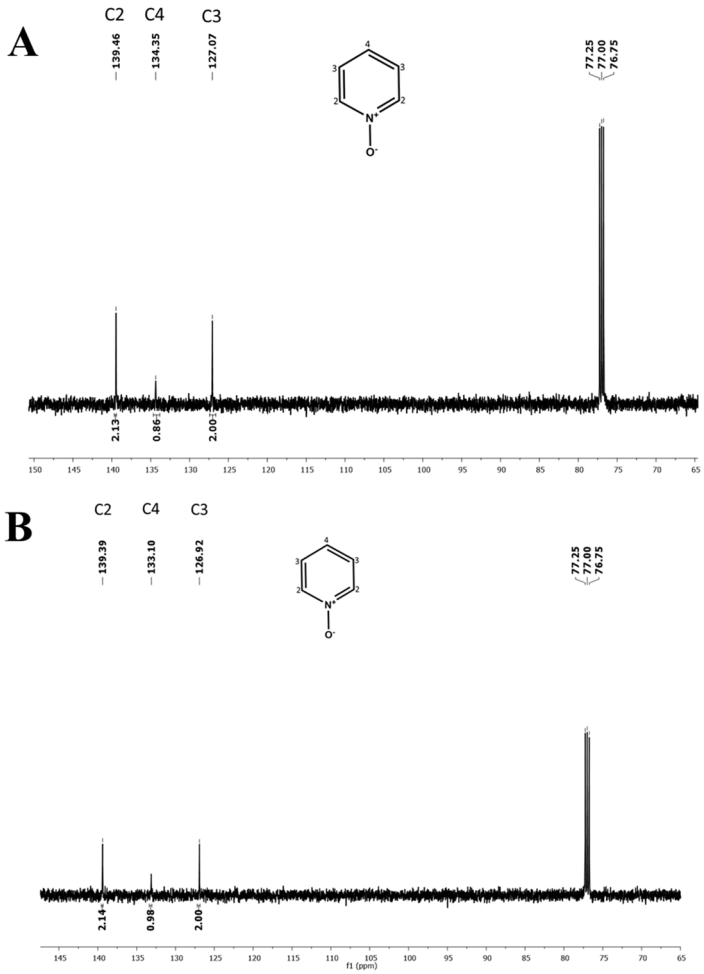

Figure 3. Representative ^{13}C NMR spectra of 250 mM PyO within DESs (La : U) at 1 : 3 (panel A) and 1 : 7 (panel B) molar ratios.

There are two highly unusual aspects associated to these probe-reported empirical parameters that clearly emerge. First and foremost, the values of polarity indicators, π^* and $\boldsymbol{E_T^N}$, are exceptionally high – they are almost the highest reported for any solvent system (π^* ranges from 1.50 to 1.70 and $\boldsymbol{E_T^N}$ from 1.29 to 1.42). In comparison, for choline chloride (ChCl)-based DESs, the reported π^* is 1.23 for (ChCl : U :: 1 : 2) [11], 1.373 for (ChCl : citric acid :: 1 : 1) [25], and 1.406 for (ChCl : $ZnCl_2$ :: 1 : 2) [25]. The highest π^* for any DES that we could find in the literature is 1.671 for (betaine : citric acid :: 1 : 1) [25] under ambient conditions. Clearly, these (lanthanide salt : urea) based DESs offer exceptionally high dipolarity/polarizability especially at compositions having high metal salt content. This further manifests in unprecedented high $\boldsymbol{E_T^N}$ values [$\boldsymbol{E_T^N}$ of 1.42 for (La : U :: 1 : 3) is the highest, and we could not find comparable $\boldsymbol{E_T^N}$ for any solvent system in the literature]. The exceptionally high probe-reported polarity of these (lanthanide salt : urea) DESs can be effectively utilized in chemical synthesis and separation along with many other applications.

Table 1. Dipolarity/polarizability (π^*) and HBA basicity (β) of (Ln : U) based DESs at 298.15 K.

DESs	Ratio	π^*	β
La : U	1 : 3	1.64	0.07
	1 : 4	1.62	0.10
	1 : 5	1.59	0.13
	1 : 6	1.54	0.19
	1 : 7	1.53	0.20
Ce : U	1 : 3.5	1.61	0.30

 doi:10.20944/preprints202405.0237.v1

	1 : 4	1.61	0.30
	1 : 5	1.58	0.33
	1 : 6	1.54	0.38
	1 : 7	1.50	0.43
Gd : U	1 : 2	1.70	-0.01
	1 : 3	1.62	0.08
	1 : 4	1.59	0.12
	1 : 5	1.58	0.13
	1 : 6	1.54	0.18
	1 : 7	1.53	0.19

Table 2. HBD acidity values (α's), E_T^N, $E_T(30)$ of the (La : U) DESs at 298.15K.

DES	Ratio	α_{24}	α_{RD}	E_T^N	$E_T(30)$
La : U	1 : 3	1.55	1.77	1.42	76.67
	1 : 4	1.51	1.71	1.39	75.64
	1 : 5	1.46	1.66	1.35	74.54
	1 : 6	1.39	1.58	1.29	72.65
	1 : 7	1.38	1.56	1.29	72.35

The second unusual aspect of the data is as follows. The decrease in π^* and E_T^N with increasing relative amount of urea is easy to comprehend as urea, the neutral constituent, is increased and lanthanide salt, the ionic constituent is decreased. However, surprisingly, α shows a decrease and β shows an increase as the HBD constituent urea is increased (and HBA salt is decreased) within the DES system. This is tentatively attributed to the presence of hydrated water in the system, which is contributing significantly to the HBD acidity, and as the relative amount of hydrated metal salt decreases, the α also decreases (while most of the urea is involved in H-bonding interaction). Slight increase in β as the relative amount of urea is increased in the DES system appears to be a complex interplay of the interactions involving salt, hydrated water, and urea. Further experimentation in our research labs are on-going to obtain insight into this observation. It is also noteworthy that for these DESs the α values are fairly high [e.g., 1.77 for (La : U :: 1 : 3)], if not the highest [> 2.00 for DESs constituted of (ChCl : D-sorbital :: 1 : 2), (ChCl : citric acid :: 1 : 1), (ChCl : lactic acid :: 1 : 1), (betaine : glycerol :: 1 : 2), (betaine : citric acid :: 1 : 1), and (betaine : urea :: 1 : 2)] [25]. Surprisingly, β values of these (lanthanide : urea) DESs are significantly lower in comparison to other DES systems [among reported β of DESs, only (ChCl : urea : ethylene glycol :: 1 : 1 : 1) (β = 0.000), (ChCl : ethylene glycol : formamide :: 1 : 1 : 1) (β = 0.000), and (betaine : citric acid :: 1 : 1) (β = 0.012) exhibit such low H-bond accepting basicity] [25].

In order to corroborate these unusually high probe-reported polarities of (lanthanide salt : urea) DESs, we explored behavior of judiciously selected fluorescence probes within these DESs. First, a wavelength-shift fluorescence probe pyrene-1-carboxaldehyde (PyCHO), which affords information about the "effective" dielectric constant (ε_{eff}) of solubilizing media [26], is used to assess the polarity of (lanthanide salt : urea) DESs. PyCHO exhibits well-structured emission band in non-polar solvents, which becomes broad structureless as polarity is increased [27]. The strong dependency of the PyCHO emission spectra on ε_{eff} is mirrored by a gradual bathochromic shift with increasing ε_{eff} of the medium [26]. As expected, the emission spectra and band maxima of PyCHO in (lanthanide salt : urea) DESs presented in Figure 4 (emission spectra for other DESs at all the investigated compositions are presented in Figure S3) show broad structureless band with gradual bathochromic shift with a decrease in the amount of urea suggesting increasing polarity (or 'effective' dielectric constant). More importantly, the emission band maxima of PyCHO in (lanthanide salt : urea) DES systems are in the range 472-486 nm (Table 3) while for other hydrophilic ChCl-based DESs the values lie in 452-460 nm range [28]. The emission maxima for these DESs particularly at lower (Ln : U) molar ratio are even higher than that reported in water (*ca.* 475 nm) [28] implying ε_{eff} of these DES systems to be higher than that of even water. These outcomes clearly demonstrate the unusually high polarity surrounding

 doi:10.20944/preprints202405.0237.v1

the probe cybotactic region for PyCHO when dissolved in these type-IV (Ln : U) DESs, and corroborate the outcomes of the empirical polarity parameters discussed above.

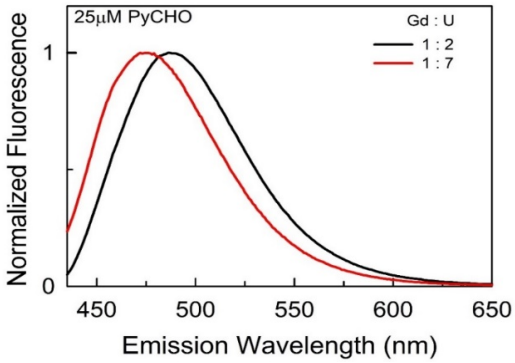

Figure 4. Representative emission spectra of 25 μM PyCHO ($\boldsymbol{\lambda_{ex} = 406\ nm}$) within DESs (Gd : U) at 1 : 2 and 1 : 7 molar ratios.

Table 3. Emission wavelength maxima ($\boldsymbol{\lambda_{max}^{em}/nm}$) of 25 μM PyCHO in (Ln : U) based DESs at 298.15 K.

Ratio	La : U	Ce : U	Gd : U
1 : 7	479	474	472
1 : 6	482	476	477
1 : 5	482	477	477
1 : 4	483	479	483
1 : 3.5		482	
1 : 3	486		484
1 : 2			486

Next, we have used one of the popular fluorescent twisted intramolecular charge-transfer (TICT) probe 9-diethylamino-5-benzo[a]phenoxazinone, commonly called as Nile red [29], which due to its planer structure and poor solubility, is known to form aggregates in aqueous (and highly polar) medium [29]. The fluorescence spectral response of Nile red reveals unique solute-solute interactions when solubilized in (lanthanide salt : urea) DESs. Most interestingly, the absorbance and excitation spectra of Nile red are different from each other; excitation maxima of the probe particularly for (Ce : U) and (Gd : U) DESs are significantly hypsochromically-shifted as compared to the absorbance maxima (Figure S4 and Table 4) clearly implying probe aggregation within these DESs. Further, the spectral maxima strongly depend on the composition of a given DES system (highlighted in Figure 5) - as compared to (Gd : U :: 1 : 2), the absorbance and excitation maxima of Nile red in (Gd : U :: 1 : 7) are significantly blue-shifted (~28 and ~25 nm, respectively). Overall, the unusual behavior of Nile red within these metal DESs indicates the formation of H-aggregates. The hypothesis of the formation of H-aggregates in DESs is further supported by the absence of the characteristic sharp bathochromically-shifted emission spectra for the J-aggregates indicating the Nile red aggregates formed within these DESs to be non-emissive H-aggregates [30]. The presence of aggregates was further confirmed using resonance light scattering (RLS). It was observed that with the increase in the concentration of Nile red, the intensity of the band at *ca.* 642 nm is increased in (Ln : U :: 1 : 7) DESs (Figure S5). The hydrophobic nature of Nile red and poor solubility in water combined with π-π stacking interactions of the planar structure contribute to its aggregation to form non-emissive H-aggregates [29,31]. We believe the exceptionally-high polarity of these DESs leads to the aggregation of Nile red in (lanthanide salt + urea) DESs. Finally, it is noteworthy that the emission maxima of Nile red varies from 658 nm to 677 nm in these DESs (Table 4), which is considerably bathochromic as compared to other DESs, ionic liquids, and polar solvents (emission maxima ≤ 580 nm) [28,32]. This enormous difference in emission maxima could be a combined effect of very high polarity of the

 doi:10.20944/preprints202405.0237.v1

(lanthanide salt : urea) DESs (leading to lower energy emission bands) and the fact that emission originates from the aggregates of the probe.

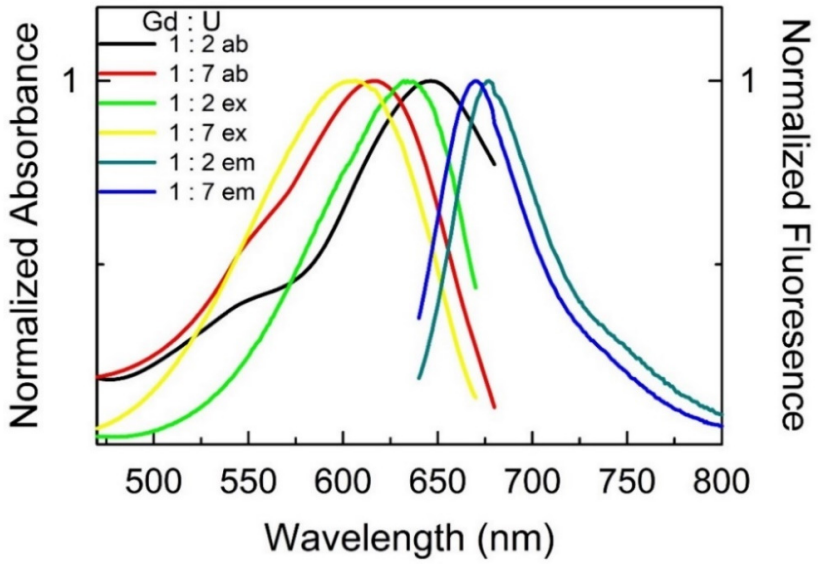

Figure 5. Representative absorbance (ab, 10 μM), excitation (ex, 25 μM), and emission (em, 25 μM) spectra of Nile red dissolved in DESs (Gd : U) at 1 : 2 and 1 : 7 molar ratios. .

Finally, we used a popular amphiphilic fluorescence probe 8-hydroxypyrene-1,3,6-trisulfonic acid (pyranine) [33], an arylsulfonate with an −OH group and planer aromatic ring that undergoes excited-state proton transfer (ESPT) depending on the environment of media [33]. This probe is highly sensitive to its cybotactic region, and depending on the polarity of the surrounding milieu, it can exist in two different forms, protonated (ROH) and deprotonated (RO^-) [34,35]. The emission spectra of pyranine in three (lanthanide salt : urea) DES systems are presented in Figure S6; representative spectra are shown in Figure 6. Based on the literature, the emission band with maxima appearing at 450 (±5) nm characterizing the excited protonated form (ROH^*) is the dominant form when relative amount of urea in the DES is less. However, increasing urea in our DES system results in appearance of a shoulder at long wavelength (*ca.* 515 nm) which is due to the emergence of deprotonated form of pyranine (RO^{-*}). The ESPT to the DES at higher relative urea amounts is further supported by the excite-state intensity decay [I(t)] measurements. The I(t) acquired at both 450 nm and 515 nm in all the investigated (Ln : U) DESs and the associated global fit decay parameters are reported in Table S2. Importantly, it is observed that at low urea concentrations, the decay fits best to a single exponential function at both wavelengths implying presence of only the ROH^*, whereas at higher urea concentrations, the decay starts to show a better fit to a double exponential decay function with one of the recovered pre-exponential factors being negative implying the process to take place after the excitation. It has been reported earlier that pyranine readily undergoes ESPT in methanol-urea mixture; as urea is increased, more-and-more RO^{-*} is formed [36]. Formation of UH^+ is proposed to facilitate the deprotonation of pyranine in its excited-state [36]. We believe increase in HBA basicity (β) of the media with increasing urea is responsible for enhanced deprotonation of pyranine as urea is increased in the DES system. Clearly, the complex interplay of high polarity and HBA basicity of (lanthanide salt : urea) DES systems controls the photophysical behavior of the probe pyranine.

 doi:10.20944/preprints202405.0237.v1

Table 4. Absorbance (λ_{max}^{ab}, 10 μM), excitation (λ_{max}^{ex}, 25 μM) and emission (λ_{max}^{em}, 25 μM) wavelength maxima of Nile red in (Ln : U) based DESs at 298.15 K.

Ratio	La : U			Ce : U			Gd : U		
	λ_{max}^{ab}/nm	λ_{max}^{ex}/nm	λ_{max}^{em}/nm	λ_{max}^{ab}/nm	λ_{max}^{ex}/nm	λ_{max}^{em}/nm	λ_{max}^{ab}/nm	λ_{max}^{ex}/nm	λ_{max}^{em}/nm
1 : 7	616	617	672	617	590	658	618	607	670
1 : 6	620	618	672	622	592	661	621	608	670
1 : 5	623	619	674	625	602	663	628	612	671
1 : 4	632	627	674	628	607	663	630	618	672
1 : 3.5				634	614	664			
1 : 3	632	631	675				636	619	675
1 : 2							646	632	677

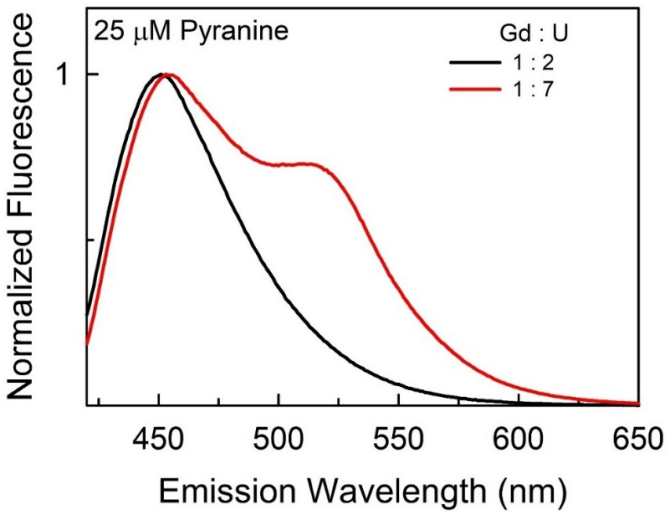

Figure 6. Representative emission spectra of 25 μM pyranine (λ_{ex} = **406 nm**) dissolved in DESs (Gd : U) at 1 : 2 and 1 : 7 molar ratios.

In order to obtain insight into the interactions between the Ln salt and urea as the DES is formed in the absence of any external probe, FTIR absorbance spectral signature of a representative DES (Gd : U :: 1 : 2) is compared with that of $Gd(NO_3)_3.6H_2O$ and urea, respectively (Figure 7 and Table S3). Significant shifts in the relevant band maxima of the Gd salt as well as urea upon formation of DES, corroborate the presence of strong interspecies interactions within the DES. These interactions appear to be responsible in affording the significantly high polarity to these DESs. In a seminal work, Edler group has reported very high surface tension and density along with low viscosity and glass transition temperatures associated to similar DESs [37]. Existence of strongly-bonded but fluxional oligomeric polyanions and polycations was put-forth. It was stated that the excess of the molecular component in the DESs resulted in intercalating H-bonded nanostructure possessing water and urea. It may be proposed that such structuring may result in highly polar cybotactic region as exhibited by the optical probes.

Preprints.org (www.preprints.org) | NOT PEER-REVIEWED | Posted: 6 May 2024 doi:10.20944/preprints202405.0237.v1

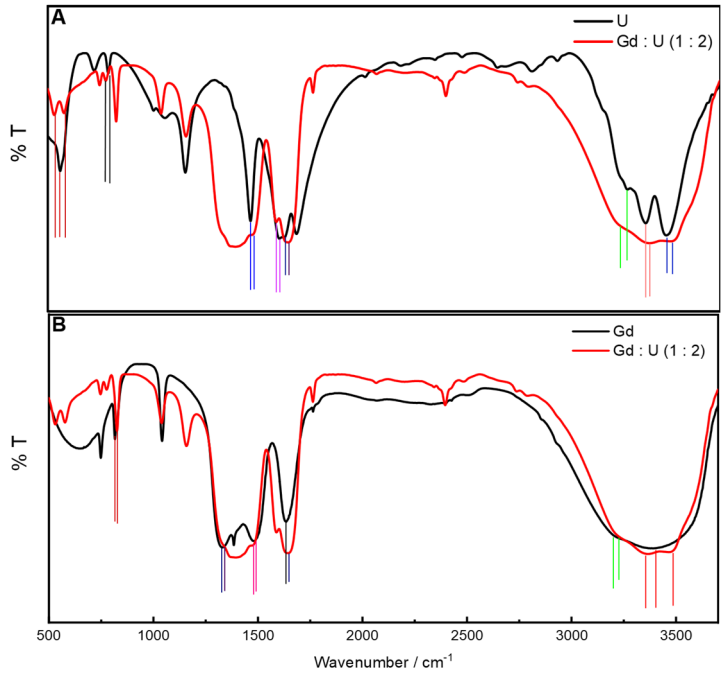

Figure 7. FTIR absorbance spectra of urea (U, panel A), $Gd(NO_3)_3.6H_2O$ (Gd, panel B), and DES (Gd : U :: at 1 : 2) (panels A and B), respectively, under ambient conditions. Vertical lines represent shift in maxima in going from the neat constituent to the DES.

4. Conclusions

We have reported our findings that DESs composed of (lanthanide salt + urea) exhibit polarity (via empirical dipolarity/polarizability, π^*, and/or $\boldsymbol{E_T^N}$ parameters, emission maxima of PyCHO, aggregation by Nile red, and prototropism by pyranine) that is higher than that of any reported solvent system in the literature especially for lanthanide salt-rich DES systems. The unusually high polarity of these DESs is attributed to the lanthanide salt as well as the hydrated water of the salt. The polarity can be effectively tuned by varying the relative amount of lanthanide salt and urea within the DES. Hydrated water of the salt, via controlling the H-bonding, plays a decisive role in controlling HBD acidity, α, and HBA basicity, β, as the composition of the DES, i.e., lanthanide salt to urea ratio, is changed. These DES systems open new avenues of applications where high cybotactic region polarity is desired.

Supplementary Materials: The following supporting information can be downloaded at the website of this paper posted on Preprints.org. Figure S1: Absorbance spectra of 20 μM DENA and 20 μM NA dissolved in Ln : U based DESs at room temperature; Figure S2: ^{13}C NMR spectra of 250 mM PyO within La : U at 1 : 4 (Panel A), 1 : 5 (Panel B) and 1 : 6 (Panel C) molar ratios; Figure S3: Fluorescence emission spectra of 25μm PyCHO ($\boldsymbol{\lambda_{ex}}$ = **406 nm**) dissolved in Ln : U based DESs at room temperature; Figure S4: Absorbance spectra of 10μM Nile red and Fluorescence excitation spectra of 25μM Nile red dissolved in Ce : U (panel A) and Gd : U (panel B) based DESs at room temperature; Figure S5: RLS spectra of Nile red with variation of concentration dissolved in Ln : U (1 : 7) based DESs at room temperature., Figure S6: Emission spectra of 25 μM pyranine ($\boldsymbol{\lambda_{ex}}$ = **406 nm**) dissolved in Ln : U based DESs at room temperature; Table S1: Absorbance wavelength ($\boldsymbol{\lambda_{max}^{ab}}$/nm) of 20 μM DENA and 20 μM NA dissolved in Ln : U based deep eutectic solvent at room temperature., Table S2: Recovered excited-state intensity decay parameters for pyranine (λ_{em} = 450 nm, 515nm; excitation with a 404 nm violet-laser diode) dissolved in the Ln : U based DES at room temperature by using global fit**;** Table S3: FTIR absorbance band maxima of urea, $Gd(NO_3)_3.6H_2O$, and DES (Gd : U) at 1 : 2 molar ratios.

Author Contributions: Conceptualization, Methodology, Visualization, Writing– original draft, Data collection, Anushis Patra; Data collection, Vaishali Khokhar; Writing– review and editing, supervision, Resources, Project administration, Siddharth Pandey.

Funding: This work is generously funded by the Council of Scientific & Industrial Research, EMR-II (CSIR-EMR-II), GoI through a grant to Siddharth Pandey [grant number 01(3043)/21/ EMR-II]. The authors gratefully acknowledge Science and Engineering Research Board (SERB), GoI for providing funding [grant no. CRG/2021/000602] for the UV-Vis spectrophotometer. We would also like to thank the Central Research Facility at IIT Delhi, for NMR measurements.

Data Availability Statement: The data presented in this study are available in the Supplementary Materials.

Acknowledgments: Anushis Patra would like to acknowledge Indian Institute of Technology, Delhi Government of India for his Senior Research Fellowship (SRF).

Conflicts of Interest: There are no conflicts to declare.

References

1. Hansen, B. B. et al. Deep Eutectic Solvents: A Review of Fundamentals and Applications. *Chem. Rev.* **2021**, *121*, 1232–1285.
2. Wagle, D. V.; Zhao, H.; Baker, G. A. Deep Eutectic Solvents: Sustainable Media for Nanoscale and Functional Materials. *Acc. Chem. Res.* **2014**, *47*, 2299–2308.
3. Liu, Y.; Friesen, J. B.; McAlpine, J. B.; Lankin, D. C.; Chen, S.-N.; Pauli, G. F. Natural Deep Eutectic Solvents: Properties, Applications, and Perspectives. *J. Nat. Prod.* **2018**, *81*, 679–690.
4. Mbous, Y. P.; Hayyan, M.; Hayyan, A.; Wong, W. F.; Hashim, M. A.; Looi, C. Y. Applications of Deep Eutectic Solvents in Biotechnology and Bioengineering—Promises and Challenges. *Biotechnol. Adv.* **2017**, *35*, 105–134.
5. Zhang, Q.; De Oliveira Vigier, K.; Royer, S.; Jérôme, F. Deep Eutectic Solvents: Syntheses, Properties and Applications. *Chem. Soc. Rev.* **2012**, *41*, 7108–7146.
6. Paiva, A.; Craveiro, R.; Aroso, I.; Martins, M.; Reis, R. L.; Duarte, A. R. C. Natural Deep Eutectic Solvents – Solvents for the 21st Century. *ACS Sustain. Chem. Eng.* **2014**, *2*, 1063–1071.
7. Zainal-Abidin, M. H.; Hayyan, M.; Ngoh, G. C.; Wong, W. F. Doxorubicin Loading on Functional Graphene as a Promising Nanocarrier Using Ternary Deep Eutectic Solvent Systems. *ACS Omega* **2020**, *5*, 1656–1668.
8. Ruesgas-Ramón, M.; Figueroa-Espinoza, M. C.; Durand, E. Application of Deep Eutectic Solvents (DES) for Phenolic Compounds Extraction: Overview, Challenges, and Opportunities. *J. Agric. Food Chem.* **2017**, *65*, 3591–3601.
9. van Osch, D. J. G. P.; Dietz, C. H. J. T.; Warrag, S. E. E.; Kroon, M. C. The Curious Case of Hydrophobic Deep Eutectic Solvents: A Story on the Discovery, Design, and Applications. *ACS Sustain. Chem. Eng.* **2020**, *8*, 10591–10612.
10. Tomé, L. C.; Mecerreyes, D. Emerging Ionic Soft Materials Based on Deep Eutectic Solvents. *J. Phys. Chem. B* **2020**, *124*, 8465–8478.
11. Pandey, A.; Pandey, S. Solvatochromic Probe Behavior within Choline Chloride-Based Deep Eutectic Solvents: Effect of Temperature and Water. *J. Phys. Chem. B* **2014**, *118*, 14652–14661.
12. Cao, J.; Su, E. Hydrophobic Deep Eutectic Solvents: The New Generation of Green Solvents for Diversified and Colorful Applications in Green Chemistry. *J. Clean. Prod.* **2021**, *314*, 127965.
13. Farooq, M. Q.; Abbasi, N. M.; Anderson, J. L. Deep Eutectic Solvents in Separations: Methods of Preparation, Polarity, and Applications in Extractions and Capillary Electrochromatography. *J. Chromatogr. A* **2020**, *1633*, 461613.
14. Khokhar, V.; Dhingra, D.; Pandey, S. Effect of Temperature and Composition on Density and Dynamic Viscosity of (Lanthanide Metal Salts + Urea) Deep Eutectic Solvents. *J. Mol. Liq.* **2022**, *360*, 119396.
15. Khalid, A.; Tahir, S.; Khalid, A. R.; Hanif, M. A.; Abbas, Q.; Zahid, M. Breaking New Grounds: Metal Salts Based-Deep Eutectic Solvents and Their Applications- a Comprehensive Review. *Green Chem.* **2024**, *26*, 2421–2453.
16. Xia, Q.; Liu, Y.; Meng, J.; Cheng, W.; Chen, W.; Liu, S.; Liu, Y.; Li, J.; Yu, H. Multiple Hydrogen Bond Coordination in Three-Constituent Deep Eutectic Solvents Enhances Lignin Fractionation from Biomass. *Green Chem.* **2018**, *20*, 2711–2721.
17. Tong, Z.; Meng, J.; Liu, S.; Liu, Y.; Zeng, S.; Wang, L.; Xia, Q.; Yu, H. Room Temperature Dissolving Cellulose with a Metal Salt Hydrate-Based Deep Eutectic Solvent. *Carbohydrate Polymers* **2021**, *272*, 118473.

18. Huo, D.; Sun, Y.; Yang, Q.; Zhang, F.; Fang, G.; Zhu, H.; Liu, Y. Selective Degradation of Hemicellulose and Lignin for Improving Enzymolysis Efficiency via Pretreatment Using Deep Eutectic Solvents. *Bioresource Technology* **2023**, *376*, 128937.
19. Chen, H.; Sun, C.; Hu, Y.; Xia, C.; Sun, F.; Zhang, Z. Reaction Characteristics of Metal-Salt Coordinated Deep Eutectic Solvents during Lignocellulosic Pretreatment. *Journal of Environmental Chemical Engineering* **2023**, *11*, 109531.
20. Khokhar, V.; Kumar, M.; Pandey, S. Pyrene Aggregation at Unprecedented Low Concentrations in (Lanthanide Metal Salt + Urea) Deep Eutectic Solvents. *Phys. Chem. Chem. Phys.* **2023**, *25*, 64–68.
21. Kamlet, M. J.; Abboud, J. L.; Taft, R. W. The Solvatochromic Comparison Method. 6. The π* Scale of Solvent Polarities. *J. Am. Chem. Soc.* **1977**, *99*, 6027–6038.
22. Madeira, P. P.; Passos, H.; Gomes, J.; Coutinho, J. A. P.; Freire, M. G. Alternative Probe for the Determination of the Hydrogen-Bond Acidity of Ionic Liquids and Their Aqueous Solutions. *Phys. Chem. Chem. Phys.* **2017**, *19*, 11011–11016.
23. Kamlet, M. J.; Taft, R.W. The Solvatochromic Comparison Method. I. The β-Scale of Solvent Hydrogen-Bond Acceptor (HBA) Basicities. *J. Am. Chem. Soc.* **1976**, *98*, 377–383.
24. Schneider, H. D.; Badrieh, Y.; Migron, Y.; Marcus, Y. Hydrogen Bond Donation Properties of Organic Solvents and Their Aqueous Mixtures from 13C NMR Data of Pyridine-N-Oxide. *Z. für Phys. Chem.* **1992**, *177*, 143–156.
25. Wojeicchowski, J. P.; Abranches, D. O.; Ferreira, A. M.; Mafra, M. R.; Coutinho, J. A. P. Using COSMO-RS to Predict Solvatochromic Parameters for Deep Eutectic Solvents. *ACS Sustain. Chem. Eng.* **2021**, *9*, 10240–10249.
26. Kalyanasundaram, K.; Thomas, J. K. Solvent-Dependent Fluorescence of Pyrene-3-carboxaldehyde and Its Applications in the Estimation of Polarity at Micelle-Water Interfaces. *J. Phys. Chem.* **1977**, *81*, 2176–2180.
27. Street, K. W.; Acree, W. E. Estimation of the Effective Dielectric Constant of Cyclodextrin Cavities Based on the Fluorescence Properties of Pyrene-3-Carboxaldehyde. *Appl Spectrosc* **1988**, *42*, 1315–1318.
28. Pandey, A.; Rai, R.; Pal, M.; Pandey, S. How Polar Are Choline Chloride-Based Deep Eutectic Solvents? *Phys. Chem. Chem. Phys.* **2014**, *16*, 1559–1568.
29. Dutta, A. K.; Kamada, K.; Ohta, K. Spectroscopic Studies of Nile Red in Organic Solvents and Polymers. *J. Photochem. Photobiol A: Chem.* **1996**, *93*, 57–64.
30. Kurniasih, I. N.; Liang, H.; Mohr, P. C.; Khot, G.; Rabe, J. P.; Mohr, A. Nile Red Dye in Aqueous Surfactant and Micellar Solution. *Langmuir* **2015**, *31*, 2639–2648.
31. Mishra, A.; Behera, R. K.; Behera, P. K.; Mishra, B. K.; Behera, G. B. Cyanines during the 1990s: A Review. *Chem. Rev.* **2000**, *100*, 1973–2012.
32. Greenspan, P.; Fowler, S. D. Spectrofluorometric Studies of the Lipid Probe, Nile Red. *J. Lipid Res.* **1985**, *26*, 781–789.
33. Tolbert, L. M.; Solntsev, K. M. Excited-State Proton Transfer: From Constrained Systems to "Super" Photoacids to Superfast Proton Transfer. *Acc. Chem. Res.* **2002**, *35*, 19–27.
34. Ireland, J. F.; Wyatt, P. A. H. Acid-Base Properties of Electronically Excited States of Organic Molecules. *Adv Phys Org Chem.* **1976**, *12*, 131–221.
35. Förster, Th. Primary Photophysical Processes. **1973**, *34*, 225–234.
36. Htun, T. Excited-State Proton Transfer in Nonaqueous Solvent. *J. Fluoresc.* **2003**, *13*, 323–329.
37. Hammond, O. S.; Bowron, D. T.; Edler, K. J. Structure and Properties of "Type IV" Lanthanide Nitrate Hydrate:Urea Deep Eutectic Solvents. *ACS Sustainable Chem. Eng.* **2019**, *7*, 4932–4940.